6852 *Inorg. Chem.* **2009**, *48*, 6852–6859
DOI: 10.1021/ic900783k

Inorganic Chemistry
Article

Dynamic Properties of a Hexadecamolybdenum Wheel: Studies in Solution and Density Functional Theory Calculations

Ali Kachmar,[†] Sébastien Floquet,*[,‡] Jean-François Lemonnier,[‡] Emmanuel Cadot,[‡] Marie-Madeleine Rohmer,[†] and Marc Bénard*[,†]

[†] *Laboratoire de Chimie Quantique, Institut de Chimie-UMR 7177, CNRS and Université de Strasbourg, 4 rue Blaise Pascal, 67000 Strasbourg, France, and* [‡] *Institut Lavoisier de Versailles, UMR 8180, University of Versailles, 45 avenue des Etats-Unis, 78035 Versailles, France*

Received April 23, 2009

Variable temperature ^{1}H NMR studies of the host−guest complex $[Mo_{16}O_{16}S_{16}(OH)_{16}(H_2O)_4(PDA)_2]^{4-}$ (**1** ; PDA^{2-} = phenylenediacetate) previously carried out in D_2O have revealed a complex behavior in solution, involving a gliding motion of both parallel phenyl rings of the PDA^{2-} ligands. In the present work, we present new NMR spectra carried out in the aprotic solvent CD_3CN, which allow the observation of the proton signals associated with the bridging hydroxo groups of the inorganic host. The new spectra provide detailed information about the concerted reorganization of the guest components, that is, PDA^{2-} and water molecules. The existence of an equilibrium between two distinct isomers differing in the linking mode between the inorganic host and the two equivalent PDA^{2-} ligands is evidenced. This equilibrium appears strongly dependent upon the temperature, leading to a complete inversion of the distribution between 300 and 226 K. The thermodynamic data related to the isomerization reaction have been determined ($\Delta_rH = -50.5$ kJ mol^{-1} and $\Delta_rS = -215$ J mol^{-1} K^{-1}). Furthermore, at low temperature, one of the isomers exists in two conformations, only differing in the H-bond network involving the inner water molecules. Density functional theory calculations were carried out to push ahead the interpretations obtained from experiment, identify the isomers of **1**, and specify the role and the positions of the guest water molecules. Among the various structures that have been calculated for **1**, three fall in a narrow energy range and should correspond to the species characterized by variable-temperature ^{1}H NMR experiments in CD_3CN. Finally, this study shows how the internal disposition of the ligands affects the ellipticity of the Mo_{16} ring which varies from one isomer to the other in the 0.73−1 range and highlights solvation of the ring as one of the key parameters for the conformational design of these flexible host−guest systems.

Introduction

Polyoxometalates (POM) represent a wide family of inorganic compounds, which are of current interest for a number of recognized applications.[1−8] In the past decade, we have derived the first members of a new family of POMs, the cyclic polyoxothiometalates (POTMs) based on the self-condensation of the $[Mo_2O_2S_2]^{2+}$ oxothiocation around templates like polycarboxylates,[9−15] and started exploring their properties. The resulting host−guest assemblies have revealed a rare dynamic flexibility or host−guest self-adaptability.[9,14] In previous studies, we notably evidenced (i) the high flexibility and versatility of the inorganic Mo-ring as a

---

*To whom correspondence should be addressed. E-mail: sebastien.floquet@chimie.uvsq.fr (S.F.), benard@chimie.u-strasbg.fr (M.B.).

(1) (a) Geletii, Y. V.; Botar, B.; Kögerler, P.; Hillesheim, D. A.; Musaev, D. G.; Hill, C. L. *Angew. Chem., Int. Ed.* **2008**, *47*, 3896–3899. (b) Sartorel, A.; Carraro, M.; Scorrano, G.; De Zorzi, R.; Geremia, S.; McDaniel, N. D.; Bernhard, S.; Bonchio, M. *J. Am. Chem. Soc.* **2008**, *130*(15), 5006–5007.

(2) Khenkin, A. M.; Neumann, R. *J. Am. Chem. Soc.* **2008**, *130*(44), 14474–14476.

(3) Proust, A.; Thouvenot, R.; Gouzerh, P. *Chem. Commun.* **2008**, No. 16, 1837–1852.

(4) AlDamen, M. A.; Clemente-Juan, J. M.; Coronado, E.; Marti-Gastaldo, C.; Gaita-Arino, A. *J. Am. Chem. Soc.* **2008**, *130*(28), 8874–8875.

(5) Mialane, P.; Dolbecq, A.; Sécheresse, F. *Chem. Commun.* **2006**, No. 33, 3477–3485.

(6) Ogata, A.; Yanagie, H.; Ishikawa, E.; Morishita, Y.; Mitsui, S.; Yamashita, A.; Hasumi, K.; Takamoto, S.; Yamase, T.; Eriguchi, M. *Br. J. Cancer* **2008**, *98*(2), 399–409.

(7) Wilson, E. F.; Abbas, H.; Duncombe, B. J.; Streb, C.; Long, D. L.; Cronin, L. *J. Am. Chem. Soc.* **2008**, *130*(42), 13876–13884.

(8) Mal, S. S.; Dickman, M. H.; Kortz, U.; Todea, A. M.; Merca, A.; Bogge, H.; Glaser, T.; Müller, A.; Nellutla, S.; Kaur, N.; van Tol, J.; Dalal, N. S.; Keita, B.; Nadjo, L. *Chem.*—*Eur. J.* **2008**, *14*(4), 1186–1195.

(9) Salignac, B.; Riedel, S.; Dolbecq, A.; Sécheresse, F.; Cadot, E. *J. Am. Chem. Soc.* **2000**, *122*(42), 10381–10389.

(10) Cadot, E.; Sécheresse, F. *Chem. Commun.* **2002**, No. 19, 2189–2197.

(11) Cadot, E.; Marrot, J.; Sécheresse, F. *Angew. Chem., Int. Ed.* **2001**, *40* (4), 774–777.

(12) Lemonnier, J.-F.; Kachmar, A.; Floquet, S.; Marrot, J.; Rohmer, M.-M.; Bénard, M.; Cadot, E. *Dalton Trans.* **2008**, No. 34, 4565–4574.

(13) Lemonnier, J.-F.; Floquet, S.; Marrot, J.; Terazzi, E.; Piguet, C.; Lesot, P.; Pinto, A.; Cadot, E. *Chem.*—*Eur. J.* **2007**, *13*(12), 3548–3557.

(14) Lemonnier, J.-F.; Floquet, S.; Kachmar, A.; Rohmer, M.-M.; Bénard, M.; Marrot, J.; Terazzi, E.; Piguet, C.; Cadot, E. *Dalton Trans.* **2007**, No. 28, 3043–3054.

(15) Floquet, S.; Marrot, J.; Cadot, E. *C. R. Chim.* **2005**, *8*(6−7), 1067–1075.

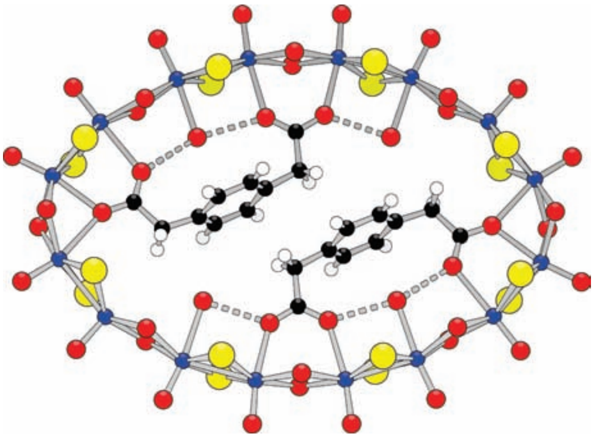

Figure 1. X-ray Molecular structure of **1**. Blue, molybdenum; yellow, sulfur; red, oxygen; black, carbon; and white, hydrogen.

Scheme 1. Postulated Dynamic Equilibrium between the Two Equivalent C_{2h} Limit Conformations of **1** in Aqueous Solution

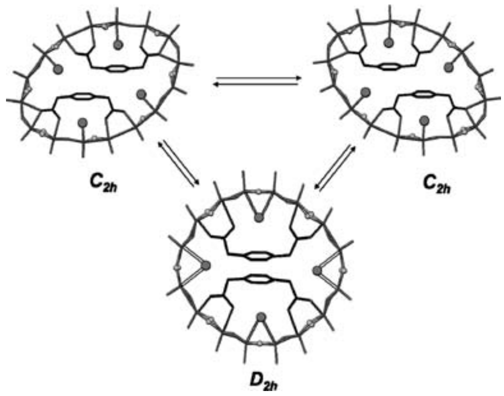

function of the embedded ligand;[14] (ii) the dynamic motions of the ligands within the Mo-wheels in solution,[9,14] and (iii) the driving force which governs the formation of the host−guest assemblies.[12] We recently demonstrated that the formation and the stability of the host−guest systems are intimately related to the conformational constraints of the encapsulated ligands but also strongly depends on the presence of weak intramolecular forces, such as van der Waals or H-bonding interactions. In this context, the compound $[Mo_{16}O_{16}S_{16}(OH)_{16}(H_2O)_4(PDA)_2]^{4-}$, hereafter abbreviated as $[Mo_{16}(PDA)_2]^{4-}$ (**1**), possesses two phenylenediacetate (PDA^{2-}) ligands which interact through CH-π contacts, and four inner aquo ligands involved within a H-bond network (Figure 1).[13] Both types of intramolecular interactions evidenced by X-ray diffraction study bring stability and robustness to the host−guest assembly. However, the linkage of each PDA^{2-} ligand to the inorganic ring is achieved by means of the attachment of one carboxylate function to two Mo atoms belonging to different $[Mo_2O_2S_2]$ units, a feature unprecedented in the family of templated polyoxothiometalates. NMR study in solution revealed that **1** is liable to adopt several positional or conformational isomers related by a dynamic process. In particular, a back-and-forth movement between two equivalent, crystal-like, mirror-image conformations was postulated in D_2O (Scheme 1). Therefore, questions arise about the pathway linking these two conformations, the involvement of the encapsulated water molecules, the energy of the transition state(s), and the possible occurrence of other metastable structures deriving from **1**. Herein, we report on the dynamic behavior of the $[Mo_{16}(PDA)_2]^{4-}$ host−guest system, guided and supported by density functional theory (DFT) calculations.

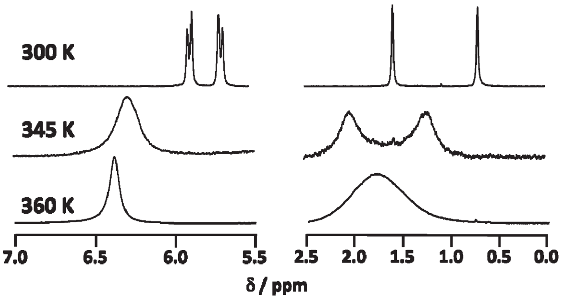

Figure 2. Variable temperature ^1H NMR spectra of **1** in D_2O.

Experimental Section

Chemicals. The synthesis of the lithium salt of the $[Mo_{16}(PDA)_2]^{4-}$ anion was carried out as previously reported[13] and checked by routine methods (FT-IR, EDX, ^1H NMR). Chemicals were purchased from Aldrich or Acros chemicals whereas deuterated solvent were purchased from Eurisotop Company.

NMR Measurements. NMR measurements were performed either in D_2O or CD_3CN on a Bruker Avance 300 operating at 300 MHz in 5 mm tubes. Chemical shifts were referenced to the usual external TMS standard. The studies in solution were carried out on the previously reported lithium salt of **1** by using variable temperature ^1H NMR in D_2O and in CD_3CN (Figures 2 and 3).

Computational Details. DFT calculations have been carried out with the 2004 version of the ADF program[16−18] using the gradient-corrected BP86 exchange-correlation functional[19−21] All atoms are described with the Slater basis sets referred to as TZP in the User's Guide. The basis set for hydrogen is triple-ζ plus one p-type orbital. For non-metal atoms, the core (He for oxygen and carbon, Ne for sulfur) is frozen and described by a single Slater function, whereas the valence set is triple-ζ and supplemented with a d-type polarization function. The small core (3s3p3d) of molybdenum was also modeled by a frozen Slater basis. The valence shell is double-ζ for 4s, triple-ζ for 4p, 4d, and 5s, and supplemented with a single Slater orbital describing the 5p shell. The geometry and the energy of the complex in solution have been modeled by means of the conductor-like screening model (COSMO) as implemented in ADF, with the dielectric constant currently used for water, $\varepsilon = 78$.[22−24] Using this value obviously models the complex solvated in water, and provides an upper limit to the solvation effects expected to arise in non-aqueous solvents. It should be noted that even in the latter case, the first solvation shell is expected to retain, as in the crystal structure, a number of water molecules forming a network of strong hydrogen bonds with the hydroxo groups.

---

(16) te Velde, G.; Bickelhaupt, F. M.; Baerends, E. J.; Fonseca Guerra, C.; van Gisbergen, S. J. A.; Snijders, J. G.; Ziegler, T. *J. Comput. Chem.* **2001**, *22*, 931–967.

(17) Fonseca Guerra, C.; Snijders, J. G.; te Velde, G.; Baerends, E. J. *Theor. Chem. Acc.* **1998**, *99*, 391–403.

(18) *ADF2004.01*; SCM, Theoretical Chemistry, Vrije Universiteit: Amsterdam, The Netherlands, 2004; http://www.scm.com.

(19) Becke, A. D. *J. Chem. Phys.* **1993**, *98*, 5648–5652.

(20) Perdew, J. P. *Phys. Rev. B* **1986**, *33*(12), 8822–8824.

(21) Perdew, J. P. *Phys. Rev. B* **1986**, *34*(10), 7406–7406.

(22) Klamt, A.; Schuurmann, G., *J. Chem. Soc., Perkin Trans. 2*, **1993**, (5), 799-805.

(23) Klamt, A. *J. Phys. Chem.* **1995**, *99*(7), 2224–2235.

(24) Model Implemented in the ADF package by Pye, C. C.; Ziegler, T. *Theor. Chem. Acc.* **1999**, *101*, 396–408.

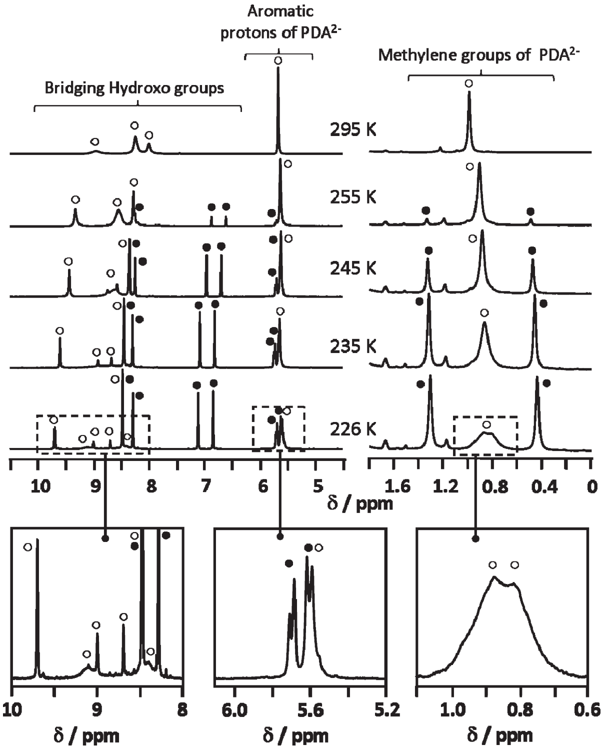

Figure 3. Variable temperature ^{1}H NMR spectra of **1** in CD_3CN. (○) $[Mo_{16}(C_{2v}\text{-}PDA)_2]^{4-}$ and (●) $[Mo_{16}(C_s\text{-}PDA)_2]^{4-}$.

Results and Discussion

Solution Studies. The ^{1}H NMR spectrum of $[Mo_{16}(PDA)_2]^{4-}$ recorded at 300 K in D_2O displays four signals with similar intensities, distributed as two single resonances at 1.58 ppm and 0.70 ppm, and two doublets of equal intensity centered at 5.85 and 5.69 ppm (see Figure 2). These NMR lines are assigned to the two equivalent PDA^{2-} ligands embedded in the Mo-ring with local C_s symmetries. This low symmetry exhibited by each PDA^{2-} ligand agrees with the molecular structure of **1** determined by X-ray diffraction and originates principally in the asymmetric anchorage mode of the ligands to the inorganic ring. Indeed, one carboxylate function bridges two Mo atoms of one $[Mo_2O_2S_2]$ building block whereas the other span two adjacent $[Mo_2O_2S_2]$ units (Figure 1). Interestingly, ^{1}H NMR spectrum of **1** in D_2O revealed a strong dependence upon temperature related to a dynamic molecular process. From 300 to 360 K, the resonances attributed to the aromatic protons and those assigned to the methylene groups collapse into two broad signals at 6.37 ppm ($\Delta\nu_{1/2}$ = 24 Hz) and 1.79 ppm ($\Delta\nu_{1/2}$ = 465 Hz) (see Figure 2). Such a result indicates that both anchored PDA^{2-} ions display at 360 K a C_{2v} local symmetry, probably averaged on the NMR time scale. Therefore, questions arise about the behavior and the role of the inorganic host toward the dynamic rearrangement of the inner components of the Mo_{16}-ring.

In aprotic solvent (CD_3CN), the ^{1}H NMR signals of the bridging hydroxo groups of the inorganic host can be observed, thus providing additional informations about the host−guest system. The ^{1}H NMR spectra of $[Mo_{16}(PDA)_2]^{4-}$ as lithium salt recorded in CD_3CN at variable temperature (295−226 K) are shown in Figure 3.

Scheme 2. Postulated Conformations of **1** in Solution[a]

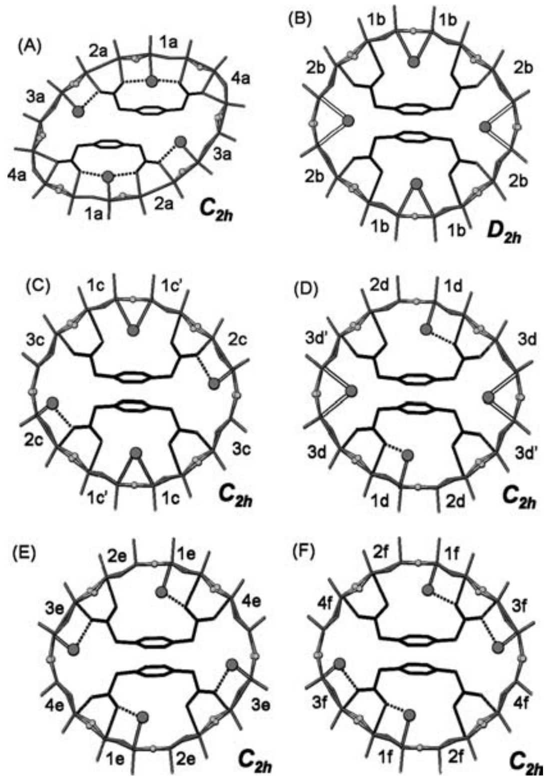

[a] The labels indicate the different types of bridging hydroxo groups. The dotted lines indicate H-bonds.

The ^{1}H NMR spectrum of $Li_4[Mo_{16}(PDA)_2]$ in CD_3CN at 295 K exhibits five resonances related to the organic and inorganic parts of the cluster. The two embedded PDA^{2-} ligands give only two resonances at 0.99 and 5.65 ppm, consistent with a symmetric anchorage mode (C_{2v} local symmetry). Such a feature clearly contrasts with that obtained in aqueous medium (see Figure 2). The three remaining broad lines found at 8.96 ($\Delta\nu_{1/2}$ = 56 Hz), 8.23 ($\Delta\nu_{1/2}$ = 21 Hz), and 7.99 ppm ($\Delta\nu_{1/2}$ = 19 Hz) with 1:2:1 intensity ratio (4H, 8H, and 4H, respectively) correspond to the hydroxo bridges of the inorganic ring. It is worth noting that such a ^{1}H NMR distribution for the resonances of the hydroxo groups disagree with any symmetry for the Mo_{16} wheel. Two, four, or eight equal signals would be expected for a Mo_{16} ring with a D_{2h}, C_{2h}, or C_s symmetry, respectively (see Scheme 2). Then, the presence of three signals should be consistent with the overlap of two lines to produce the 8H intensity resonance at 8.23 ppm. In addition, there is an apparent discrepancy between the observed C_{2v} local symmetry of the two equivalent PDA^{2-} groups and the resonances of the hydroxo groups. The coexistence in the same complex of two equivalent PDA^{2-} ions with C_{2v} local symmetry, however, require the highest D_{2h} symmetry for the overall host−guest system, in contradiction with spectroscopic evidence at 295 K.

Upon varying temperature from 295 to 226 K in CD_3CN, the NMR spectra evidence several features. First, the pattern of the initial spectrum does not change significantly until 265 K, except that among the three peaks assigned to the hydroxo groups, the two 4H signals sharpen and the single 8H signal broadens. As usually observed, a gradual variation of the chemical shifts is observed toward the high frequency domain.[9,14] Below 265 K, a new set of peaks grows reversibly and becomes predominant at 226 K. These signals of equal intensity are distributed as four sharp resonances at 6.84, 7.11, 8.28, and 8.47 ppm, two doublets at 5.69 and 5.60 ppm, and two single lines at 1.31 and 0.44 pm corresponding to the hydroxo bridges, the aromatic protons, and the methylene groups, respectively. Such an overall distribution appears consistent with a C_{2h} frozen symmetry and could be related to the molecular structure supposed in D_2O at 300 K and to the solid state structure (see Figure 1 and Scheme 2A). Such an isomer contains two equivalent PDA^{2-} ligands with a local C_s symmetry and will be denoted hereafter $[Mo_{16}(C_s\text{-}PDA)_2]^{4-}$.

Concomitantly with the appearance of $[Mo_{16}(C_s\text{-}PDA)_2]^{4-}$, the five resonances observed at 295 K significantly change below 255 K. The broad NMR line observed at 8.23 ppm (at 295 K) splits at 226 K to give rise to four signals distributed as two sharp components at 9.00 and 8.69 ppm and two broad signals at 9.10 and 8.40 ppm (Figure 3). At the same time, the NMR lines of hydroxo groups at 8.96 and 7.99 ppm at 295 K appear only shifted and sharpened at low temperature (9.49 and 8.47 ppm). Deconvolution and relative integration of the six resulting lines give 1.0/0.65/0.35/0.35/1.0/0.65. Finally, the singlet assigned to the aromatic protons of PDA^{2-} ligands is not modified in the 295−226 K range, while the resonance of the methylene groups observed as a single line at 295 K splits into two close components at 226 K ($\Delta\nu_{1/2}$ = 57 Hz). These intricate changes indicate that both equivalent PDA^{2-} display a quasi symmetrical anchorage mode (pseudo C_{2v} symmetry). The distribution of the hydroxo resonances (six lines) with nonequivalent integration is consistent with the presence of two frozen conformations, but some accidental degeneracies have to be involved necessarily. Especially, the two sharp lines at 9.69 and 8.47 ppm at 226 K with the same intensity should be the result of accidental degeneracies of two distinct resonances. Then, this part of the low temperature spectrum should be interpreted as two frozen conformations in 65/35 proportion with formal C_{2h} symmetries. It is likely that the accidental degeneracies observed either for the hydroxo groups or for the PDA^{2-} components are related to close local chemical environments of the involved nuclei. Consequently, full explanation of the ^1H NMR spectrum of the $[Mo_{16}(PDA)_2]^{4-}$ system at low temperature leads to postulate three different arrangements, one being consistent with the solid state structure, while the other two would appear intimately correlated and rather consistent with global C_{2h} symmetries where both PDA^{2-} display a symmetrical anchorage mode and a pseudo C_{2v} symmetry, therefore abbreviated $[Mo_{16}(C_{2v}\text{-}PDA)_2]^{4-}$.

Finally, the present study hence evidence a temperature-dependent equilibrium, reversible and slow at the NMR time scale, between two positional isomers, that is, $[Mo_{16}(C_{2v}\text{-}PDA)_2]^{4-}$ and $[Mo_{16}(C_s\text{-}PDA)_2]^{4-}$. The change from one form to the other involves a reorganization of the coordination of PDA^{2-} ligands and of the attached water molecules to the inorganic ring, resulting in a modification of the local symmetry of the ligands. The proportions of both conformations as a function of temperature are given in Figure 4.

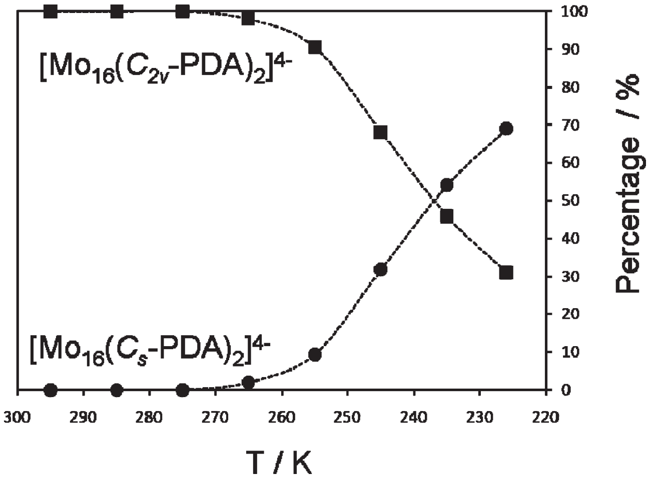

Figure 4. Speciation curve between $[Mo_{16}(C_s\text{-}PDA)_2]^{4-}$ and $[Mo_{16}(C_{2v}\text{-}PDA)_2]^{4-}$ in CD_3CN as a function of temperature.

An equilibrium constant K_{eq} corresponding to the ratio ($[Mo_{16}(C_s\text{-}PDA)_2]^{4-}/[Mo_{16}(C_{2v}\text{-}PDA)_2]^{4-}$) can be deduced from these data, and the associated thermodynamic parameters are calculated between 260 and 226 K as $\Delta_rH = -50.5$ kJ mol^{-1} and $\Delta_rS = -215$ J K^{-1}mol^{-1} ($\Delta_rH = -12.1$ kcal mol^{-1} and $\Delta_rS = -51.4$ cal K^{-1}mol^{-1}). The Gibbs' energy corresponding to such an isomerization process reveals an inversion of distribution between both isomers below T = 238 K. Thus, the $[Mo_{16}(C_s\text{-}PDA)_2]^{4-}$ appears to be stabilized only under frozen conditions (T < 238 K) in CD_3CN, while this species is predominant at T = 300 K in D_2O. The enthalpic contribution could reflect the coordination modes of the PDA^{2-} ions within the ring, while the origin of the entropy decrease could be related to the distribution of the internal water molecules. Nevertheless, to support the overall hypotheses, DFT calculations have been carried out and reported in the following section.

DFT Calculations. DFT calculations have been carried out on various forms of the host−guest complex $(H_2O)_n@[Mo_{16}O_{16}S_{16}(OH)_{16}(PDA)_2]^{4-}$ (n = 0, 4), belonging to different symmetry point groups, to delineate the influence of the coordination mode of the PDA^{2-} ligands and that of the intramolecular water molecules on the host−guest bond energy and on the dynamic processes occurring in water and in non-aqueous solvents. Bond energies ΔE between the inorganic host and the guest molecules (PDA^{2-} and water) have been derived from a difference between the energy optimized for the complex and those optimized for the isolated fragments, in their most stable configuration, as shown below for the tetrahydrated species:

$$\Delta E = E_{\text{opt}}(\text{complex}) - 2E_{\text{opt}}(\text{PDA}^{2-}) - E_{\text{opt}}[(\text{H}_2\text{O})_4] \qquad (1)$$

The reference configuration optimized for the water tetramer was that of a cyclic cluster linked via four hydrogen bonds, the second hydrogen of each molecule alternately pointing up and down the cycle. The calculated stabilization with respect to 4 isolated water molecules amounts 28.3 kcal mol^{-1}. Four configurations of PDA^{2-} were found to correspond to distinct minima

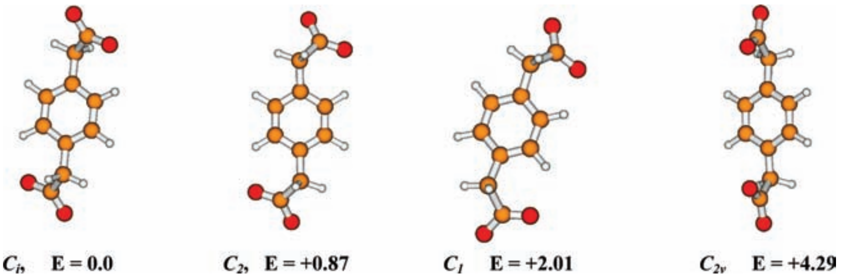

Figure 5. Four configurations optimized for PDA^{2-}, with their symmetry and their relative energies (kcal mol^{-1}).

Table 1. $[Mo_{16}(PDA)_2]^{4-}$ and $(H_2O)_4@[Mo_{16}(PDA)_2]^{4-}$: Total Bond Energy E (with Respect to Atoms) of the Complex, Either in the Gas Phase, or in Aqueous Solution (eV); Bond Energies ΔE of the PDA^{2-} and Water Ligands to the Complex; Relative Energies E_{rel} (kcal mol^{-1}) Calculated for the Various Conformations of $(H_2O)_4@[Mo_{16}(PDA)_2]^{4-}$ with Respect to the Form Observed in the Crystal; and Fragment Activation Energies E_{adjust} of the Mo_{16} and $(PDA)^{2-}$ Moieties (kcal mol^{-1})

complex	symmetry	E (gas) eV	ΔE kcal mol^{-1}	E_{rel} kcal mol^{-1}	$E_{adjust}[Mo_{16}]$ kcal mol^{-1}	E_{adjust}[guests] kcal mol^{-1}	E (solvated) eV	E_{rel} (solv.) kcal mol^{-1}
$[Mo_{16}(PDA)_2]^{4-}$	C_{2h}	−833.36	−119.1		117.5	20.8		
$[Mo_{16}(PDA)_2]^{4-}$	D_{2h}	−833.91	−131.8		90.7	12.4		
$(H_2O)_4@[Mo_{16}(PDA)_2]^{4-}$	C_i^a	−891.22	−129.3	0.0	103.8	23.4	−908.36	0.0
$(H_2O)_4@[Mo_{16}(PDA)_2]^{4-}$	D_{2h}^b	−890.22	−106.3	+23.0	86.4	14.3	−907.05	+30.2
$(H_2O)_4@[Mo_{16}(PDA)_2]^{4-}$	C_2^c	−891.40	−133.5	−4.2	90.5	14.3	−908.52	−3.7
$(H_2O)_4@[Mo_{16}(PDA)_2]^{4-}$	C_i^d	−891.28	−130.7	−1.4				
$(H_2O)_4[Mo_{16}(PDA)_2]^{4-}$	D_2^e	−891.81	−143.0	−13.7	83.6	14.0	−907.92	+10.1

[a] Water molecules encapsulated in the average plane of the inorganic cycle (optimized from the observed structure, Figure 6A, Scheme 2A). [b] Eclipsed PDA^{2-} ligands; water molecules encapsulated in symmetric positions with respect to the carboxylate groups (Figure 6B, Scheme 2B); [c] Water oxygens close to the average plane of the inorganic cycle; PDA^{2-} ligands close to eclipsed position, reduced symmetry constraints (Figure 6C, Scheme 2E); [d] Same as the previous configuration, but water oxygens linked two by two to the same carboxylate end (Figure 6D, Scheme 2F); [e] Eclipsed PDA^{2-} ligands; water molecules out of the inorganic cycle (Figure 6E).

(Figure 5). As a guest molecule in complex **1**, the dicarboxylate adopts the destabilized configuration with C_{2v} symmetry, which is best adapted to coordinate the inorganic ring from the inside. Finally, DFT investigations previously carried out on complexes involving a dodecamolybdate host have shown that the inorganic ring is quite flexible and easily undergoes elliptic deformation.[14] Similar results were obtained with the $[Mo_{16}]$ cycle, for which the energy variations remain in the range of 1 kcal mol^{-1} for ellipticities varying from 1.0 (D_{4h} symmetry) to 0.73 (D_{2h} symmetry, close to the observed structure).

An important factor to consider for interpreting the relative stabilities of the complexes is the cost of the mutual adaptability between the molecular moieties, which is the energy E_{adjust} required to activate these fragments into the geometry they display in the optimized complex. It is obtained by taking the difference between the energy calculated for the considered fragment, (i) assumed isolated in the geometry optimized for the complex, and, (ii) in its optimal geometry.

Finally, the influence of aqueous solvation on the structure and dynamic behavior of the tetrahydrated complex **1** was conjectured from the geometry reoptimization of the molecule using the COSMO polarizable continuum model, with a dielectric constant $\varepsilon = 78$.[22,23] The energy values computed for various configurations of $[Mo_{16}O_{16}S_{16}(OH)_{16}(PDA)_2]^{4-}$ and $(H_2O)_4@[Mo_{16}O_{16}S_{16}(OH)_{16}(PDA)_2]^{4-}$ are displayed in Table 1.

It should be noted first that the eclipsed position of the ligand aromatic cycles, corresponding to a high D_{2h} symmetry and to the anchorage of all carboxylate functions to single $Mo_2O_2S_2$ units, is preferred when no water molecules are present, either inside or outside the molecular cage. The energy difference with respect to the equilibrium geometry derived from the observed structure amounts 12.7 kcal mol^{-1}. This is to be compared with two calculations carried out at the same level of theory on an inorganic cycle templated by a planar terephthalate ligand, $[Mo_{12}O_{12}S_{12}(OH)_{12}(O_2C-C_6H_4-CO_2)]^{2-}$. One of the computed forms corresponded to the observed structure, in which both carboxylate functions bridge single $Mo_2O_2S_2$ units, and the other to a hypothetic one in which both COO^- groups are shifted by one Mo atom and therefore bridge two different metal−metal bonded dimers. The energy of the second form was found higher by 11.2 kcal mol^{-1}. It therefore seems that the displacement of each COO^- function across the bridging hydroxo ligands is made at a cost of ~6 kcal mol^{-1}. Furthermore, in the present case, the mutual adaptability of the host and the guests in the structure with C_{2h} symmetry requires an additional and important destabilizing contribution from all fragments (Table 1), which is, however, compensated in part by stronger coordinative bonds, with shorter Mo−O distances, and by some relief in the steric repulsion between the PDA^{2-} ligands.

Encapsulating four water molecules inside the inorganic cycle or allowing them to lie in close vicinity to the carboxylate functions drastically modifies the relative stabilities between the configurations with full D_{2h} and full C_{2h} symmetries, not considering in the latter case those protons of the water molecules which are pointing outside the molecular plane and break the C_{2h} symmetry

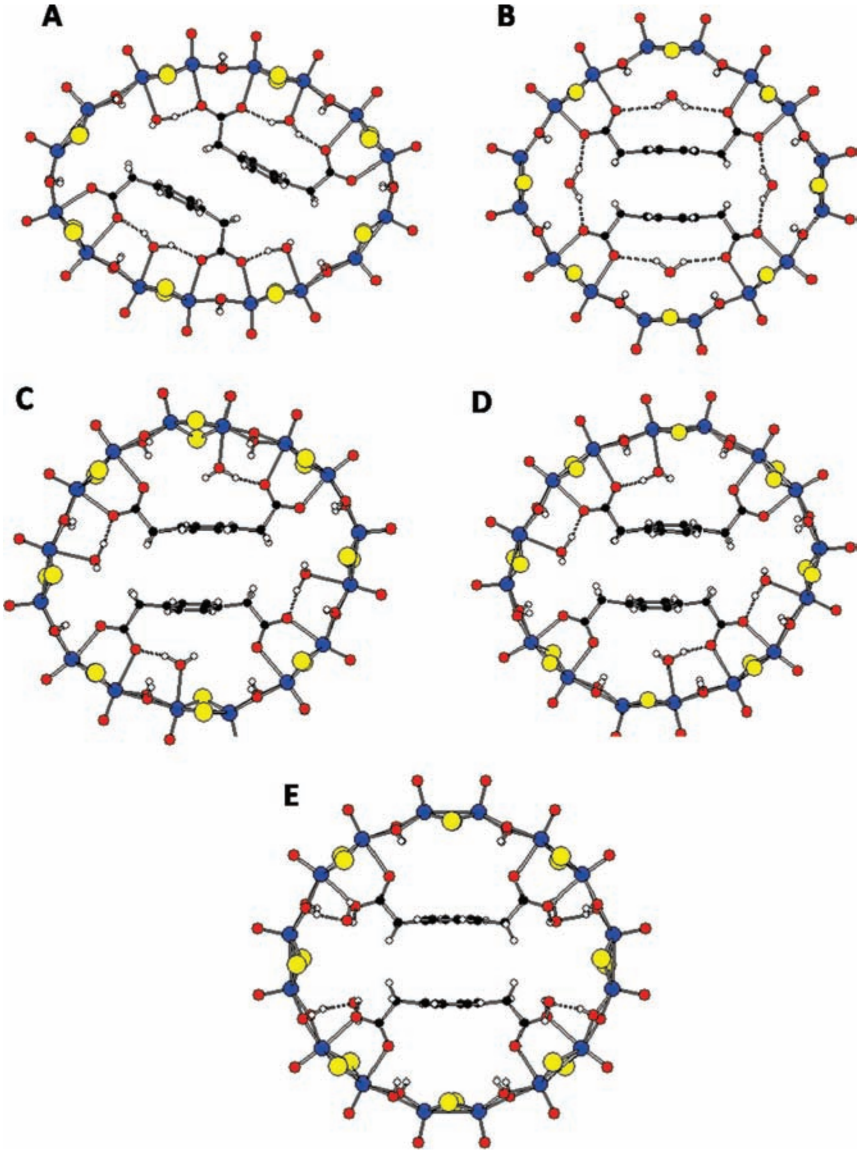

Figure 6. Representation of the configurations optimized from DFT for $(H_2O)_4[Mo_{16}(PDA)_2]^{4-}$ (A) with staggered PDA^{2-} ligands and C_{2h} symmetry, similar to the observed structure and to Scheme 2A; (B) with eclipsed PDA^{2-} ligands and D_{2h} symmetry (Scheme 2B); (C) with approximately eclipsed PDA^{2-} ligands, deduced from structure B by a concerted clockwise shift of the 4 water molecules (Scheme 2E); (D) with approximately eclipsed PDA^{2-} ligands, deduced from structure C by the swing of two water molecules between two PDA^{2-} ligands (Scheme 2F); (E) with eclipsed PDA^{2-} ligands and out-of-plane water molecules (D_2 symmetry).

into C_i (Table 1). Varying the positions of these four water molecules inside and outside the molecular plane also introduces many more conformational possibilities and provides some insight into the interpretation of the variable temperature NMR spectra.

It first appears from the bond energies ΔE (Table 1) that the encapsulation of four water molecules stabilizes the observed C_{2h} configuration by 10.2 kcal mol^{-1} (Figure 6A). Let us remember that this increase of $-\Delta E$ is computed with respect to a water tetramer strongly stabilized not only with H-bonds involving sequential pairs of molecules but also with interactions between non-nearest neighbors. The extra stabilization calculated for **1** therefore emphasizes the strength of the hydrogen bonds involving a carboxylate oxygen. However, a large part of this interaction vanishes when the tetra-hydrated complex is constrained to a strict D_{2h} symmetry: the $H\cdots O$ distances become too large, either inside or outside the PDA^{2-} ligands, to provide more than a weak electrostatic attraction. The configuration with D_{2h} symmetry (Figure 6B) is therefore destabilized with respect to the observed form, by 23 kcal mol^{-1} in the gas phase and by 30 kcal mol^{-1} in solution. Furthermore, the D_{2h}-constrained configuration is unstable with respect to a concerted shift of the four water molecules toward one specific carboxylate oxygen. The most favorable shift is uniformly (counter)clockwise, yielding each carboxylate to bind one single water molecule, either on the internal or on the external side of the ligand (Figure 6C). The symmetry of the complex breaks into C_{2h} if water oxygens only are considered, into C_2 or C_i when protons are taken into account. It is found slightly more stable than the configuration observed in the crystal phase, by 4.2 kcal mol^{-1} in the gas phase and by 3.7 kcal mol^{-1} in solution. Even though the aromatic cycles of the ligands remain close to an eclipsed conformation, a slight shift has been induced by the clockwise displacement of the four water molecules (Figure 6C).

Another configuration can be deduced from the unstable D_{2h} form by shifting the water molecules in opposite directions, which yields one carboxylate group free of water on each PDA^{2-} ligand, whereas the other groups are attached to two water molecules (Figure 6D). This configuration is expected to arise when temperature increases from the wagging movement of the two water molecules most labile inside the complex.

These mobile water molecules are expected to lie outside the pockets formed by the PDA^{2-} ligands, since the O$\cdots$O distances between two proximate ligand oxygens calculated in the most stable eclipsed configuration (Scheme 2C) are somewhat closer between different carboxylate units (5.99 Å) than between two functions of the same ligand (6.57 Å). Let us notice, however, that the configuration in which two water molecules are linked through H-bonds to the same carboxylate group (Figure 6D, Scheme 2F) is less stable by 2.8 kcal mol^{-1} than the one resulting from a balanced distribution of the H-bonds among the anionic ends (Figure 6C, Scheme 2E). The residence time of the water molecules in the latter form is therefore expected to be larger. Taking into account the probable occurrence of configurations with intermediate stability in which only one carboxylate in the complex attaches two water molecules, calculation therefore allows understanding the NMR data acquired in CD_3CN and especially the nature of $[Mo_{16}(C_{2v}\text{-}PDA)_2]^{4-}$.

Calculations versus Experiments. DFT calculations reveal two isomers, differing by the ellipticity of the inorganic host (see Figure 6). The existence of these isomers has been postulated for the interpretation of the ^1H NMR spectra in CD_3CN. The high temperature species, which splits into two arrangements at low temperature is consistent with the PDA-eclipsed isomer. DFT calculation shows that this species produces several distributions for the four inner water molecules. According to the NMR results supported by DFT calculations, the highest symmetry can be ruled out. However, less symmetrical arrangements related to the presence of the four aquo ligands within the PDA-eclipsed ring were found. These arrangements differ only by their inner H-bond network and consequently, only slight changes are expected from the nominal D_{2h} symmetry. At T = 295 K, the NMR spectrum in CD_3CN is consistent with an average structure based on the arrangements 6C and 6D (2E and 2F in Scheme 2), both being related by the fast hopping of the water molecules on their adjacent coordination sites. On the basis of NMR observations at T = 295 K, the fast hopping must involve only two equivalent water molecules leading to the average structures 2C or 2D (see Scheme 2). Examination of the optimized geometries of structures 2C and 2D reveals that the distances between the adjacent coordination sites differ enough to propose as more probable the arrangement 2D. As previously shown, the chemical shifts of the hydroxo groups are mainly sensitive to the binding mode of the inner component (water molecules or carboxylate groups). Four possible arrangements, retaining C_{2v} symmetry and including the labeled hydroxo groups are depicted in Scheme 2C–F. The arrangements 2C and 2D could be invoked to understand the ^1H NMR spectrum in CD_3CN at 295 K. Both contain two pairs of hydroxo groups, labeled {1c, 1c′} and {3d, 3d′} which exhibit close local environments. These nearly equivalent protons should display close chemical shifts and thus give rise to an accidental degeneracy consistent with the resonance at 8.23 ppm ($\Delta\nu_{1/2}$ = 21 Hz). Furthermore, among both arrangements, only 2D reflects the nearly equivalent local environment of the methylene groups and aromatic protons of the PDA^{2-} ligands. In other words, the origin of the symmetry decreasing from D_{2h} (Scheme 2B) to C_{2v} (Scheme 2D) lies only in the presence of two singly coordinated water molecules which affect only the resonances of the hydroxo groups close to these water molecules, that is, hydroxo groups labeled 1d and 2d. It is worth noting that the 2D arrangement has to correspond to an average dynamic position where the two bridging water molecules are the result of a fast hopping on the two closest coordination sites. This is experimentally evidenced since the temperature decreasing down to 226 K cancels the water dynamics to give two frozen conformations, consistent with the arrangements 2E and 2F (see Scheme 2). The cancellation of the water hopping on the NMR time scale affects strongly the signal assigned to the protons 3d and 3d′ which split into into two pairs of twin peaks with “high” and “low” integration values, related to the 2E and 2F deduced arrangements. To a lesser extent, the signal of the methylene groups in the vicinity of the oscillating water molecules also splits into two close resonances.

Let us finally notice that the eclipsed conformation is calculated more stable than the staggered one either in the gas phase or in solution. However, the energy difference remains weak, namely, of the order of 4 kcal mol^{-1} (Table 1), which remains compatible with the interpretation of the NMR data in solution suggesting a change of conformation with temperature.

As far as the complex is assumed isolated, the most stable configuration of $(H_2O)_4[Mo_{16}(PDA)_2]^{4-}$ does not encapsulate the four water oxygen atoms inside the inorganic ellipse. Pulling the water molecules outside the average molecular plane without breaking the hydrogen bonds with the four carboxylates reduces the strain on the inorganic ring (Table 1) and provides additional hydrogen contacts between each water molecule and a hydroxo bridge. This strengthened hydrogen bond network seems to prevail over the loss of the coordinative bond of water molecules and eventually gives rise to relative stabilization energies of 13.7 and 9.5 kcal mol^{-1} with respect to the most stable forms with encapsulated water and with staggered or eclipsed conformations of $(PDA^{2-})_2$, respectively (Table 1). However, simulations carried out with COSMO show that the stabilization provided by these four, out-of-plane, individual water molecules is adequately taken into account by the solvation model. COSMO indeed restores the two equilibrium configurations with encapsulated water molecules as the most stable ones, with an energy difference similar to that obtained in the gas phase, whereas the form with the individualized water molecules placed outside the molecular plane becomes relatively *destabilized* by 10.1 and 13.8 kcal mol^{-1}, respectively (Table 1). However, the position of these out-of-plane water molecules in the immediate vicinity of the carboxylate groups and the extension they provide to the network of hydrogen bonds involving these functions suggests that they could take part in the dynamic process characterized in aqueous solvent (Scheme 1) by exchanging their positions with those of the four water molecules encapsulated in the inorganic ring.

Summary and Conclusion

A joint theoretical and NMR study of the polyoxothiometalate complex $(H_2O)_4@[Mo_{16}O_{16}S_{16}(OH)_{16}(PDA)_2]^{4-}$ (**1**) has evidenced the existence in CD_3CN solution of a temperature-dependent, dynamic equilibrium between two structures, one characterized by the staggered conformation of the PDA^{2-} ligands observed in crystal phase (Scheme 2A), and another one in which the two dicarboxylates are almost eclipsed, when the elliptic deformation of the inorganic ring has been reduced (conformations 2E and 2F at low temperature, averaged 2D conformation above 255 K). The thermodynamic parameters associated to the isomerization process ($\Delta_r H = -12.1$ kcal mol^{-1} and $\Delta_r S = -51.4$ cal K^{-1} mol^{-1}) is related to the changes of the coordination mode of the PDA^{2-} ligands and the distribution of the inner aquo ligands within the cavity. In the eclipsed form, the NMR spectra and the calculations confirm that the carboxylate groups bridge Mo atoms belonging to a single $[Mo_2O_2S_2]$ building block. The staggered form, characterized by an asymmetric coordination mode of the dicarboxylate ions, leads to a loss of stability estimated to ~ 6 kcal mol^{-1} per site. Furthermore, calculations emphasize the importance of the water molecules encapsulated in the complex and the strength of the H-bond network they establish with carboxylate groups for defining the structure of the stable conformers and for designing the dynamic processes which occur either in D_2O or CD_3CN solvents. These results highlight the solvation of the ring as one of the key parameters for the conformational design of these host−guest flexible systems.

Acknowledgment. DFT calculations have been carried out at the CINES Computer Centre (Montpellier, France) with a grant of computer time from GENCI (Paris, France).

Supporting Information Available: Cartesian coordinates of the various structures optimized for $(H_2O)_n@[Mo_{16}O_{16}S_{16}(OH)_{16}(PDA)_2]^{4-}$ (n = 0,4). This material is available free of charge via the Internet at http://pubs.acs.org.